Short Communication

Telocytes reduce oxidative stress by downregulating DUOX2 expression in inflamed lungs of mice

Haihong Tang[1,2,†], **Tao Liang**[3,†], **Yile Zhou**[1,†], **Huihui Ju**[1], **Dongli Song**[4,*], **and Hao Fang**[1,5,*]

[1]Department of Anesthesiology, Zhongshan Hospital, Fudan University, Shanghai 200032, China, [2]Department of Anesthesiology, Jinshan Hospital, Fudan University, Shanghai 201508, China, [3]Department of Anesthesiology, Shanghai East Hospital, Tongji University, Shanghai 200120, China, [4]Zhongshan Hospital Institute for Clinical Science, Shanghai Xuhui Central Hospital, Zhongshan-Xuhui Hospital, Zhongshan Hospital of Fudan University, Shanghai 200032, China, and [5]Department of Anesthesiology, Minhang Hospital, Fudan University, Shanghai 201199, China
[†]These authors contributed equally to this work.
*Correspondence address. Tel: +86-13817826329; E-mail: drfanghao@163.com (H.F.) / Tel: +86-13917765916; E-mail: songdongli37@126.com (D.S.)

Abstract

Telocytes (TCs), a novel type of interstitial cells, have been found to participate in tissue protection and repair. In this study, we investigated the antioxidative effects of TCs in inflamed lungs of mice. Acute respiratory distress syndrome (ARDS) mice were used as models of inflamed lungs of mice. Gene sequencing was used to screen the differentially expressed miRNAs in TCs after lipopolysaccharide (LPS) stimulation. AntagomiR-146a-5p-pretreated TCs were first injected into mice, and antioxidant activity of TCs was estimated. TCs, RAW264.7 cells, and MLE-12 cells were collected for the detection of expressions of NOX1–4, DUOX1–2, SOD1–3, GPX1–2, CAT, Nrf2, miR-146a-5p, and miR-21a-3p after LPS stimulation. Silencing miRNAs were delivered to examine the involved signaling pathways. Oxidative stress was examined by measuring malondialdehyde (MDA) levels. We found that microRNA-146a-5p and microRNA-21a-3p were upregulated in TCs after LPS stimulation. ARDS mice that were preinfused with TCs had lower lung tissue injury scores, lung wet-dry ratios, white blood cell counts in alveolar lavage fluid and lower MDA concentrations in lung tissue. However, in antagomiR-146a-5p-pretreated ARDS mice, the infusion of TCs caused no corresponding changes. After LPS stimulation, DUOX2 and MDA concentrations were downregulated in TCs, while DUOX2 was restored by antagomiR-146a-5p in TCs. Dual-luciferase reporter assay confirmed that CREB1 was downregulated by miR-146a-5p, while DUOX2 was downregulated by CREB1, which was confirmed by treating TCs with a specific CREB1 inhibitor. This study demonstrates that LPS stimulation upregulates miR-146a-5p in TCs, which downregulates the CREB1/DUOX2 pathway, resulting in a decrease in oxidative stress in cultured TCs. TCs reduce LPS-induced oxidative stress by decreasing DUOX2 in inflamed lungs of mice.

Key words telocyte, miR-146a-5p, DUOX2, oxidative stress, cAMP-response element-binding protein 1

Introduction

Acute respiratory distress syndrome (ARDS) is an acute clinical symptom characterized by diffuse alveolar cell damage and severe injury of the respiratory alveolo-capillary barrier followed by non-cardiogenic pulmonary edema and hypoxic dyspnea, due to widespread inflammation in the lungs [1–4]. Enhanced oxidative stress is an important mechanism underlying the development of ARDS [5,6]. It was reported that ARDS patients have higher levels of hydrogen peroxide in their breath than healthy subjects [7,8]. In pulmonary tissue, oxidative stress reduces the formation of alveolar

surfactants, leading to a collapse of alveoli. Antioxidant treatments reduce the leakage of bronchoalveolar lavage and mitigate pulmonary edema in LPS-induced lung injury [9].

In the structure of lung telocytes (TCs), a novel type of interstitial cells were described soon after their discovery in 2010 [10,11]. These peculiar cells, characterized by uncommon cellular extensions called telopodes, were characterized in many organs [12,13]. Among these localizations, the presence of TCs has been reported in the myocardium [14], gastrointestinal tract [15,16], lungs [17,18] and kidneys where TCs were shown to exert protective effects in

acute kidney injury [19], infected lung [20] as well as infarcted myocardium [21]. Lung TCs have been extensively investigated by genomic and proteomic studies, which reveal that TCs can be differentiated from other cell types found in the lung parenchyma, such as fibroblasts, endothelial cells, pneumocytes, airway cells, mesenchymal stem cells (MSCs), and lymphocytes [22–24]. The therapeutic roles of TCs in the respiratory tract were hypothesized from the beginning, and one important role in the reduction of inflammation in experimental astma was demonstrated after transplantation of TCs, which could improve allergen-induced asthma by obviously inhibiting airway inflammation and airway hyper-responsiveness preclinically, with the down-regulation of Th2-related cytokine IL-4, transcription factor GATA-3 and Th2 cell differentiation, and the up-regulation of Th1-related cytokine IFN-γ, transcription factor T-bet and Th1 cell proliferation in asthma [25]. Our previous study demonstrated that TCs increase MSC migration in the attempt to treat experimental acute lung injury [26]. Moreover, co-cultivation of TCs with other cells, like stem cells, exert important effects. We found that VEGF, IL-6 and some chemokines stimulated by IL-6 signalling are secreted by cardiac TCs and overexpressed in co-cultures with cardiac stem cells (CSCs). The expression levels of MIP-2 and MIP-1α were increased by 2 folds and 4 folds, respectively, when TCs were co-cultured with CSCs, while the expression of IL-2 did not significantly differ between TCs and CSCs in mono culture but significantly decreased by 2 folds in the co-culture system. These data suggest that the TC secretome plays a modulatory role in stem cell proliferation and differentiation [27], and this may also be important for the lung.

In our previous study, we found that exogenous TCs protect against LPS-induced pulmonary injury by reducing cytokine levels [20] and promoting angiogenesis [28]. In the *in vitro* experiments, TCs were co-cultured with primary human dermal microvascular endothelial cells (HDMECs) as well as mouse fibroblast cells (L929), and the results showed that TCs significantly reduced LPS-induced oxidative stress [29], indicating that they have antioxidative features. However, the antioxidant role of TCs in LPS-induced lung injury has not been extensively explored. A previous study in 2019 on a lung telocyte cell-line transformed with Simian vacuolating virus 40 small and large T antigen (SV40) showed that the proliferative capacity of TCs[SV40] declined with the increase of LPS or TNFα concentration, similar to the responses of primary TCs [30]. Therefore, we hypothesized that lung TCs[SV40] may be a useful tool in the development of challenging new therapies.

MicroRNAs (miRNAs), which are small noncoding ribonucleic acid molecules, regulate target genes by inhibiting mRNA translation or promoting mRNA degradation. Moreover, miRNAs have been found in the extracellular vesicles released by TCs, both *in vitro* and *in vivo* [31,32]. It has been reported that miRNAs regulate reactive oxygen species (ROS) in cardiovascular disease [33]. MicroRNA-146a-5p regulates DUOX2 expression through both signal transducer and activator of transcription 1 (STAT1) [34] and cAMP-response element-binding protein 1 (CREB1) [35]. Previous study in our lab demonstrated that LPS stimulation increases the expressions of miR-146a-5p and miR-21a-3p in TCs [28] which takes part in the regulation of target genes by inhibiting mRNA translation or promoting mRNA degradation [36,37].

In the present study, we aimed to investigate the antioxidative effects of TCs in the inflamed lungs of mice, with a special focus on the underlying mechanisms of noncoding RNAs functioning on the enzymes involved in oxidative stress in TCs.

Materials and Methods
Reagents and antibodies
LPS was purchased from Sigma (St Louis, USA). Antibodies against CREB1 (ab31387) and phosphorylated CREB1 (ab32096) were purchased from Abcam (Cambridge, USA). Antibody against DUOX2 (NB110-61576ss) was purchased from NOVUS (Centennial, USA). Specific inhibitors of CREB1, KG-501 (HY-103299) and 666-15 (HY-101120) were purchased from MedChem Express (MCE, Monmouth Junction, USA), Lipofectamine RNAiMAX was purchased from Thermo Fisher Scientific (Rockford, USA). Bicinchoninic acid assay (BCA) kit, RIPA lysis buffer, and loading buffer were purchased from Beyotime (Shanghai, China).

Cell cultures
Mouse lung TCs were kindly provided by Dr Xiangdong Wang (Biomedical Research Center, Zhongshan Hospital, Fudan University, Shanghai, China), and cells were transfected with SV40 large and small T antigen to constructed TCs[SV40] [38]. TCs[SV40] cells were cultured in Dulbecco's modified Eagle's medium/F12 (DMEM/F12; Thermo Fisher Scientific) supplemented with 10% fetal calf serum (FBS; Thermo Fisher Scientific). Mouse RAW264.7 and MLE-12 cells were obtained from Zhongqiao Tech (Shanghai, China). All the cells were cultured in DMEM/F12. HEK293T cells (CRL-11268; ATCC, Manassas, USA) were cultured in DMEM high glucose medium (Hyclon, Gaithersburg, USA) for the Dual luciferase reporter assay [39].

Cell transfection
Cell transfection was performed using Lipofectamine RNAiMAX (Thermo Fisher Scientific) according to the manufactory's protocol. In brief, 50 nM antagomiR-146a-5p (Cat. 20000158; Ribo Biotech, Guanzhou, China) was prepared in a serum-free and antibiotic-free medium. After transfection, TCs were supplied with full growth medium until confluence. For animal experiments, TCs ($1 × 10^6$ cells) were freshly prepared in 100 μL PBS.

Animal experiments
Twenty-four male C57BL/6 mice (8 weeks old, 22–25 g) were obtained from the Shanghai SLAC Animal Company (Shanghai, China) and kept in a pathogen-free condition. The mice were housed in standard air-conditioned rooms (22–24°C) under a 12/12 h light/dark cycle, with free access to food and water. Mice were randomly divided into four groups: the control group, LPS stimulation group, TCs treatment group challenged with LPS, and miR-146a-5p-silenced TCs treatment group challenged with LPS. The mouse ARDS model was established by perfusing mice with LPS (5 mg/kg) via the trachea. TCs ($1 × 10^6$ cells) transfected with antagomiR-146a-5p or not, were administered via the tail vein 2 h before the LPS stimulation. The animals were sacrificed, and the lungs and bronchoalveolar lavage fluid were collected 24 h after the establishment of the mouse ARDS model.

All animal experments were performed following the bioethics guidelines and were approved by the Institutional Animal Care and Use Committee of Zhongshan Hospital, Fudan University (Shanghai, China).

Assessment of lung injury
To collect white blood cells in bronchoalveolar lavage fluid, mice

lungs were perfused with ice-cold phosphate-buffered saline (PBS). After centrifugation at 3000 g, white blood cells were counted under a microscope (JapanBX43; Olympus, Tokyo, Japan). The left lung was fixed in 10% formalin solution and embedded in paraffin for hematoxylin and eosin (H&E) staining. The right lung was collected to assess edema by the ratio of wet weight/dry weight (W/D) of the lung after incubation in a 60°C oven for 48 h. The lung injury was evaluated using a modified lung injury histological scoring system [38]. In brief, lung injury was scored on a scale of 0–4 using the average score of the following items: (I) alveolar capillary congestion, (II) hemorrhage, (III) infiltration of neutrophils into the airspace or the vessel wall and thickness of the alveolar wall, and (IV) alveolar wall thickness/hyaline membrane formation. A score of 0 represents normal findings, and scores between 1–4 represent the following levels of lung injuries: 1, mild lung injury (<25% lung involvement); 2, moderate lung injury (25%–50% lung involvement); 3, severe lung injury (50%–75% lung involvement); and 4, very severe lung injury (>75% lung involvement). The cytokines levels of IL-1, IL-6, and TNF-α in bronchoalveolar lavage fluid were detected by Bio-Plex Pro Mouse Cytokine 23-Plex Assay on the Bio-Rad MAGPIX Multiplex Reader (Bio-Rad, Hercules, USA).

Reverse transcription-polymerase chain reaction
Total RNA was extracted from cultured TCs using Trizol reagent (TaKaRa, Shiga, Japan). MicroRNAs were reversely transcribed with a Bulge-Loop miRNA qRT-PCR Starter kit (Ribo Biotech), and mRNAs were reversely transcribed to complementary DNA (cDNA) using a PrimeScript RT Reagent kit with gDNA Eraser (TaKaRa). Both miRNAs and mRNAs were amplified on an ABI 7500 sequence detection system (Applied Biosystems, Foster, USA). The expression levels of miR-21a-3p (Cat. MQPS0002615) and miR-146a-5p (Cat. MQPS0002462) were normalized with *U6* and mRNAs expressions were normalized with *GAPDH*. Primers used in the present study were synthesized by Sangon Biotech (Shanghai, China) as listed in Table 1.

Western blot analysis
Cultured cells were lysed in RIPA buffer containing protease inhibitors (Roche, Indianapolis, USA), phosphatase inhibitors (Beyotime), and phenylmethanesulfonyl fluoride (PMFS; Beyotime). Total protein concentration was determined using the bicinchoninic

acid assay kit (Beyotime). Samples (30 μg) were subject to SDS-PAGE and then transferred onto polyvinylidene fluoridewere (PVDF) membranes. Mebranes were blocked with 5% bovine serum albumin in Tris-buffered saline containing 0.1% Tween 20. The membranes were then incubated with primary antibody at 4°C for overnight. On the second day, the membranes were further incubated with an HRP-conjugated anti-rabbit IgG secondary antibody (1:2000; CST-7074; Cell Signaling Technology, Danvers, USA) for 1 h. Finally, target protein signals were visualized with Omni-ECL Femto Light Chemiluminescence kit (EpiZyme, Shanghai, China) on a Fluorescent Image Detection System (Tanon-52Multi; Tanon, Shanghai, China). The related signals were quantified using ImageJ software and normalized with GAPDH. The information of all the antibodies are shown as follows: antibodies against JAK1 (CST-3344), JAK2 (CST-3230), JAK3 (CST-8827), TYK2 (CST-14193), STAT1 (CST-14994), STAT2 (CST-72604), STAT3 (CST-30835), STAT4 (CST-2653), STAT5 (CST-94205), STAT6 (CST-5397), phosphorylated JAK1 (CST-74129), phosphorylated JAK2 (CST-8082), phosphorylated JAK3 (CST-5031), phosphorylated TYK2 (CST-68790), phosphorylated STAT1 (CST-7649), phosphorylated STAT2 (CST-4441), phosphorylated STAT3(Try705) (CST-9145), phosphorylated STAT3 (Ser727) (CST-9134), phosphorylated STAT5 (CST-4322), phosphorylated STAT6 (CST-9316), and GAPDH (CST-5558) were purchased from Cell Signaling Technology.

Dual luciferase reporter assay
The PHY-881 reporter vector (Hanyin Biotechnology, Shanghai, China) was used to construct the luciferase reporter vector plasmids PHY-881-WT-CREB1-3′-UTR and PHY-881-Mut-CREB1-3′-UTR. The plasmids CREB1-WT or CREB1-Mut were co-transfected with miR-146a-5p mimic (Cat. 10000158; Ribo Biotech) or negative control (Cat. 0000001; Ribo Biotech) into human embryonic kidney (HEK293T) cells using Lipofectamine 2000 reagent (Thermo Fisher Scientific). A dual-luciferase reporter assay system (Promega, Madison, USA) was used to assess luciferase activity after 24 h of transfection. Relative firefly luciferase activity was normalized to renilla luciferase activity.

Malondialdehyde (MDA) assay
Malondialdehyde levels in TCs and culture medium were measured using malondialdehyde (MDA) assay kit (S0131; Beyotime) ac-

Table 1. Sequences of primers used in this study

Gene	Forward (5′→3′)	Reverse (5′→3′)
NOX1	GGTTGGGGCTGAACATTTTTTC	TCGACACACAGGAATCAGGAT
NOX2	TGTGGTTGGGGCTGAATGTC	CTGAGAAAGGAGAGCAGATTTCG
NOX3	CAACGCACAGGCTCAAATGG	CACTCTCGTTCAGAATCCAGC
NOX4	CCAAATGTTGGGCGATTGTGT	CAGGACTGTCCGGCACATAG
DUOX1	AAAACACCAGGAACGGATTGT	AGAAGACATTGGGCTGTAGGG
DUOX2	AAGTTCAAGCAGTACAAGCGAT	TAGGCACGGTCTGCAAACAG
SOD1	GGAACCATCCACTTCGAGCA	CCCATGCTGGCCTTCAGTTA
SOD2	TTCTGGACAAACCTGAGCCC	GTCACGCTTGATAGCCTCCA
SOD3	CCTTCTTGTTCTACGGCTTGC	TCGCCTATCTTCTCAACCAGG
GPX1	AGTCCACCGTGTATGCCTTCT	GAGACGCGACATTCTCAATGA
GPX2	AAGTGTGACGTCAATGGGCA	TGAGGGAGAACGGGTCATCA
CAT	AGCGACCAGATGAAGCAGTG	TCCGCTCTCTGTCAAAGTGTG
GAPDH	GTTCAACGGCACAGTCAAG	GCCAGTAGACTCCACGACAT

cording to the manufacturer's instructions. Briefly, culture medium or cell lysates were incubated in MDA working solution at boiling temperature for 15 min. The MDA concentration was determined by measuring the absorbances at 532 nm, and normalized with protein concentrations in culture medium or cell lysates, respectively.

Statistical analysis

Data were presented as the mean ± standard deviation. The data were analyzed using the GraphPad Prism software (GraphPad Software, LaJolla, USA). One-way analysis of variance (ANOVA) was used for comparison. $P < 0.05$ was considered statistically significant.

Results

AntagomiR-146a-5p deminishes the lung protection role of exogenous TCs in LPS-induced ARDS

In our previous studies, microarray sequencing was performed to identify differential expressions of genens [28]. Here we showed that LPS significantly increased the expressions of miR-146a-5p and miR-21a-3p in TCs (Figure 1A,B). The ARDS model was established by LPS instillation [36,37]. TCs reduced the score of lung tissue injury (Figure 1C,D), W/D ratio of the lung, number of white blood cells, and cytokine concentration in alveolar lavage fluid in ARDS mice (Figure 1D). However, when being transfected with antagomiR-146a-5p, TCs failed to exert any protective effects on LPS-stimulated ARDS mice (Figure 1C,D).

AntagomiR-146a-5p decreases oxidative stress both *in vitro* and *in vivo*

MDA is the product of lipid oxidative stress, and it is correlated with the severity of oxidative stress. The MDA level was found to be increased in the lung tissue of ARDS mice, but decreased in the TCs-treated group mice, and increased again when infused with TCs pretreated with antagomiR-146a-5p (Figure 2A). MDA levels in TCs and culture media were decreased after treatment with LPS, and restored when being pretreated with antagomiR-146a-5p (Figure 2B,C). Both KG-501 and 666-15 reduced the MDA level in TCs pretreated with antagomiR-146a-5p (Figure 2B,C).

MiR-146a-5p decreases oxidative stress through DUOX2 in TCs

To find out the enzymes involved in TCs protection, both RAW264.7 and MLE-12 cells were used in the present study. RAW264.7 cells were accumulated in the lung of ARDS mice, while MLE-12 cells which are the pulmonary epithelial cells, were destroyed in ARDS mice. In the cultured RAW264.7 cells, LPS stimulation significantly increased mRNA expressions of oxidative enzyme NADPH oxidases 1 (NOX1), NOX2, dual oxidase 1 (DUOX1), and DUOX2, but significantly decreased mRNA expressions of antioxidant enzymes superoxide dismutase 3 (SOD3), glutathione peroxidase 1 (GPX1), GPX2, and catalase (CAT) (Figure 3A). In MLE-12 cells, LPS significantly increased mRNA expressions of DUOX2 and SOD3, but significantly reduced the expressions of NOX1 and NOX2 (Figure 3A). In TCs, LPS significantly increased SOD2 and SOD3 mRNA expressions, but significantly reduced NOX2, NOX3, NOX4, and DUOX2 mRNA expressions (Figure 3A). Meanwhile, MDA levels were increased in both RAW264.7 and MLE-12 cells but reduced in TCs after stimulation with LPS (Figure 3B). Since *DUOX2* is the candidate gene distinguishing TCs from
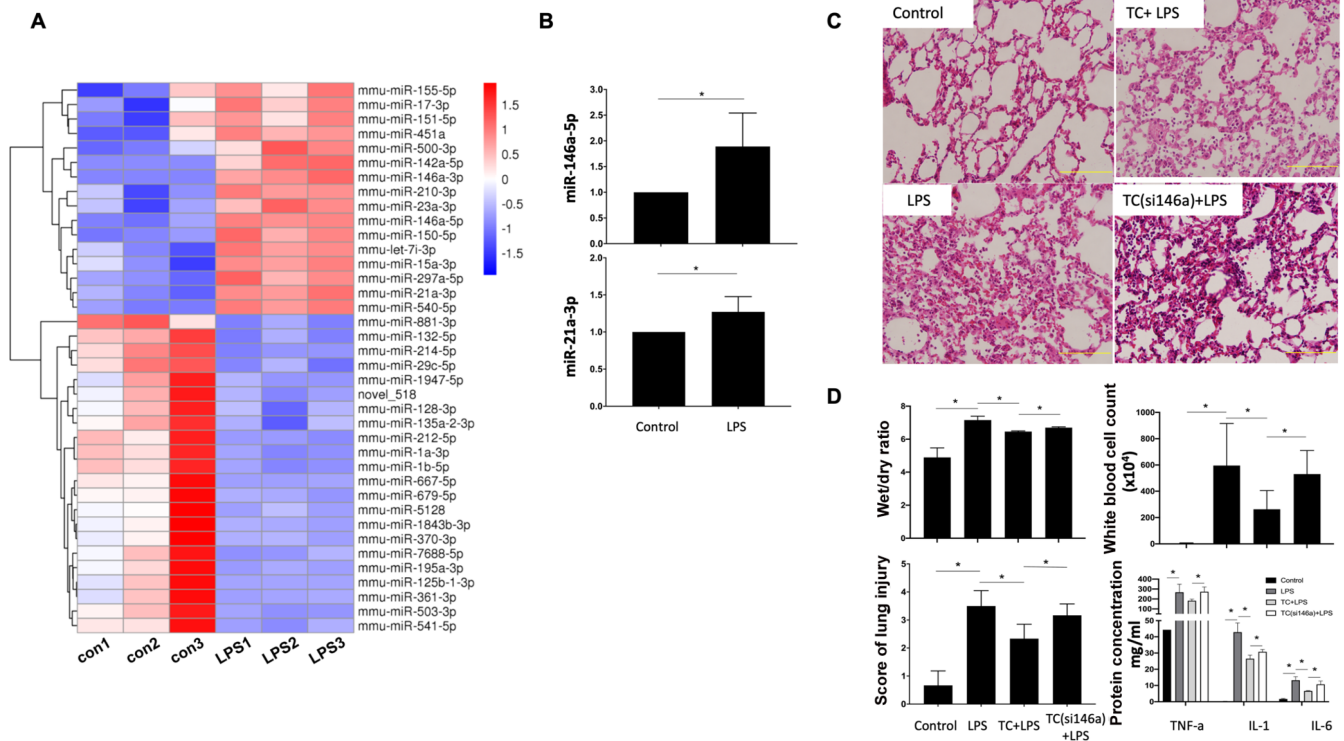

Figure 1. MiR-146a-5p in TCs plays an essential lung protection role in the mouse ARDS model (A) Heat map of differentially-expressed miRNAs in cultured TCs stimulated with LPS. (B) LPS significantly increased the expressions of miR-146a-5p and miR-21a-3p in TCs. (C,D) Compared with ARDS mice, TC-treated ARDS mice had a reduced lung tissue injury score, a lower W/D ratio of the lung, fewer white blood cells, and lower concentrations of cytokines in alveolar lavage fluid. However, when being silenced with antagomiR-146a-5p, TCs failed to exert any protective effects on LPS-stimulated ARDS mice. Data are shown as the mean ± standard deviation from six independent experiments (n = 6). *$P < 0.05$.
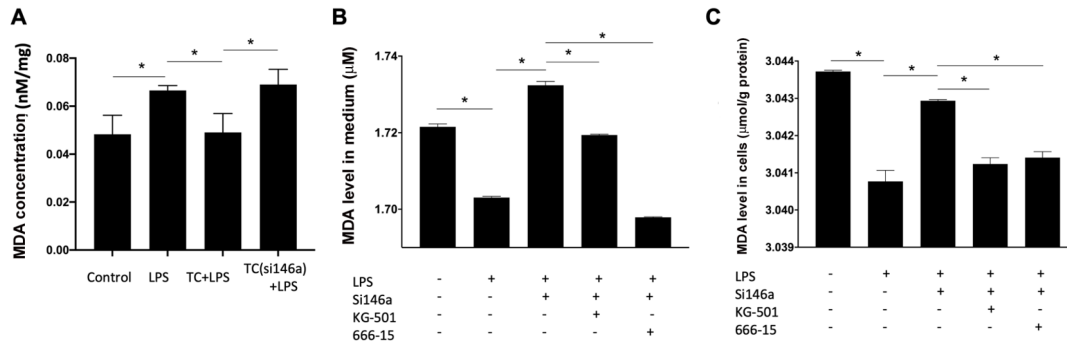
Figure 2. MiR-146a-5p in TCs decreases oxidative stress both *in vitro* and *in vivo* (A) MDA levels in the lung tissue of ARDS mice were increased, and decreased in the telocyte-treated group. MDA levels were increased again when infused with telocytes pretreated with antagomiR-146a-5p. (B, C) MDA levels in the TCs and culture media were decreased when treated with LPS, and increased again when treated with antagomiR-146a-5p. Both KG-501 and 666-15 reduced the MDA level in TCs silenced with antagomiR-146a-5p. Data are shown as the mean ± standard deviation from six independent experiments ($n = 6$). *$P < 0.05$.
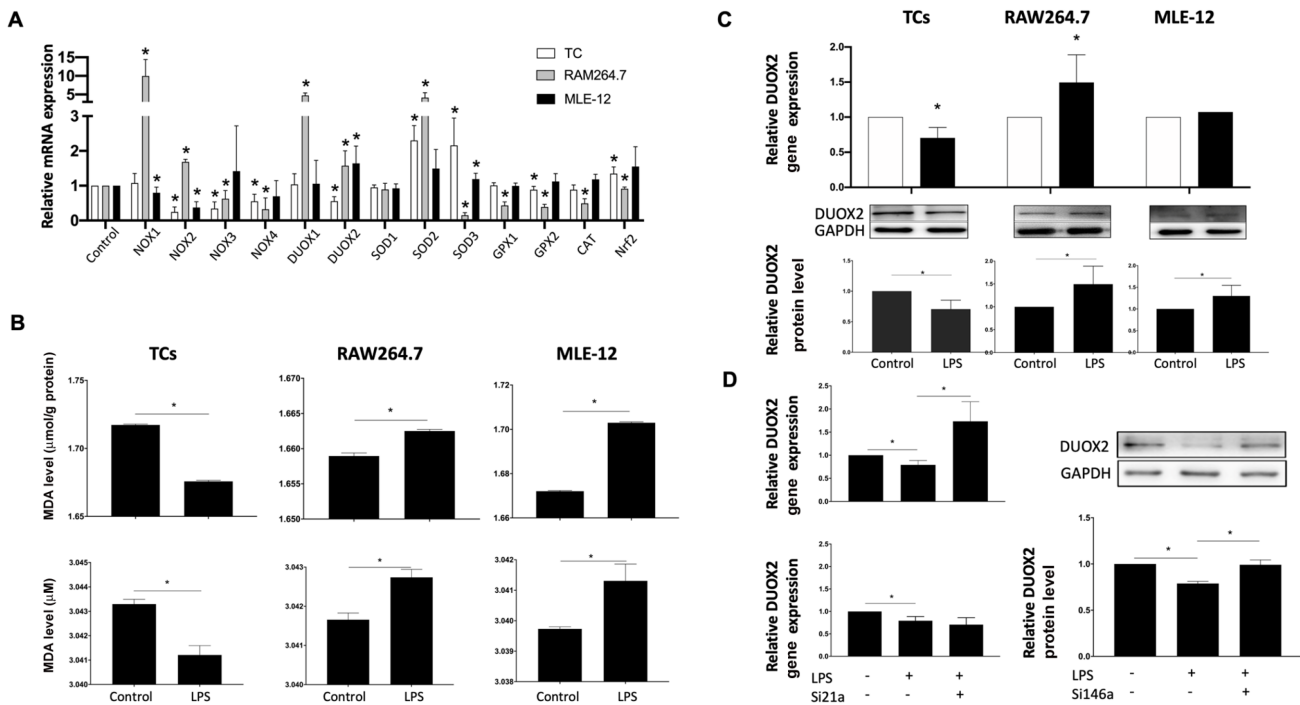

Figure 3. MiR-146a-5p in telocytes decreases oxidative stress through the DUOX2 pathway (A) The screening results of the enzymes involved in TC protection. (B) LPS increased MDA levels in both RAW264.7 and MLE-12 cells but reduced MDA levels in TCs. (C) DUOX2 was downregulated in TCs after LPS stimulation at both the mRNA and protein levels compared with those in RAW264.7 and MLE-12 cells. (D) Silencing of miR-146a-5p, but not miR-21a-3p, upregulated DUOX2 mRNA and protein expressions in TCs stimulated with LPS. Data are shown as the mean ± standard deviation from six independent experiments ($n = 6$). *$P < 0.05$.

RAW264.7 and MLE-12, DUOX2 protein expression was measured in the three cells stimulated with LPS. DUOX2 protein level was significantly increased in RAW264.7 and MLE-12 cells but significantly reduced in TCs after treatment with LPS (Figure 3C). Silencing of miR-146a-5p, but not miR-21a-3p upregulated the mRNA and protein expressions of DUOX2 in TCs stimulated with LPS (Figure 3D).

MiR-146a-5p regulates the expression of DUOX2 through CREB1 in TCs

The expression of CREB1 in TCs was decreased after treatment with

LPS, and increased when TCs were pretreated with antagomiR-146a-5p. LPS significantly reduced CREB1 protein expression, both phosphorylated protein and total protein. AntagomiR-146a-5p restored CREB1 expression in the presence of LPS (Figure 4A). Dual-luciferase reporter assay revealed that miR-146a-5p mimic significantly reduced wild-type *CREB1* promoter activity in HEK293T cells, but not in HEK293T cells with mutated *CREB1* (Figure 4B). AntagomiR-146a-5p significantly increased DUOX2 protein expression in TCs when compared with cells transfected with the negative control. In the presence of antagomiR-146a-5p and LPS, the pharmacological inhibitors of CREB1, KG-501 and 666-15, significantly
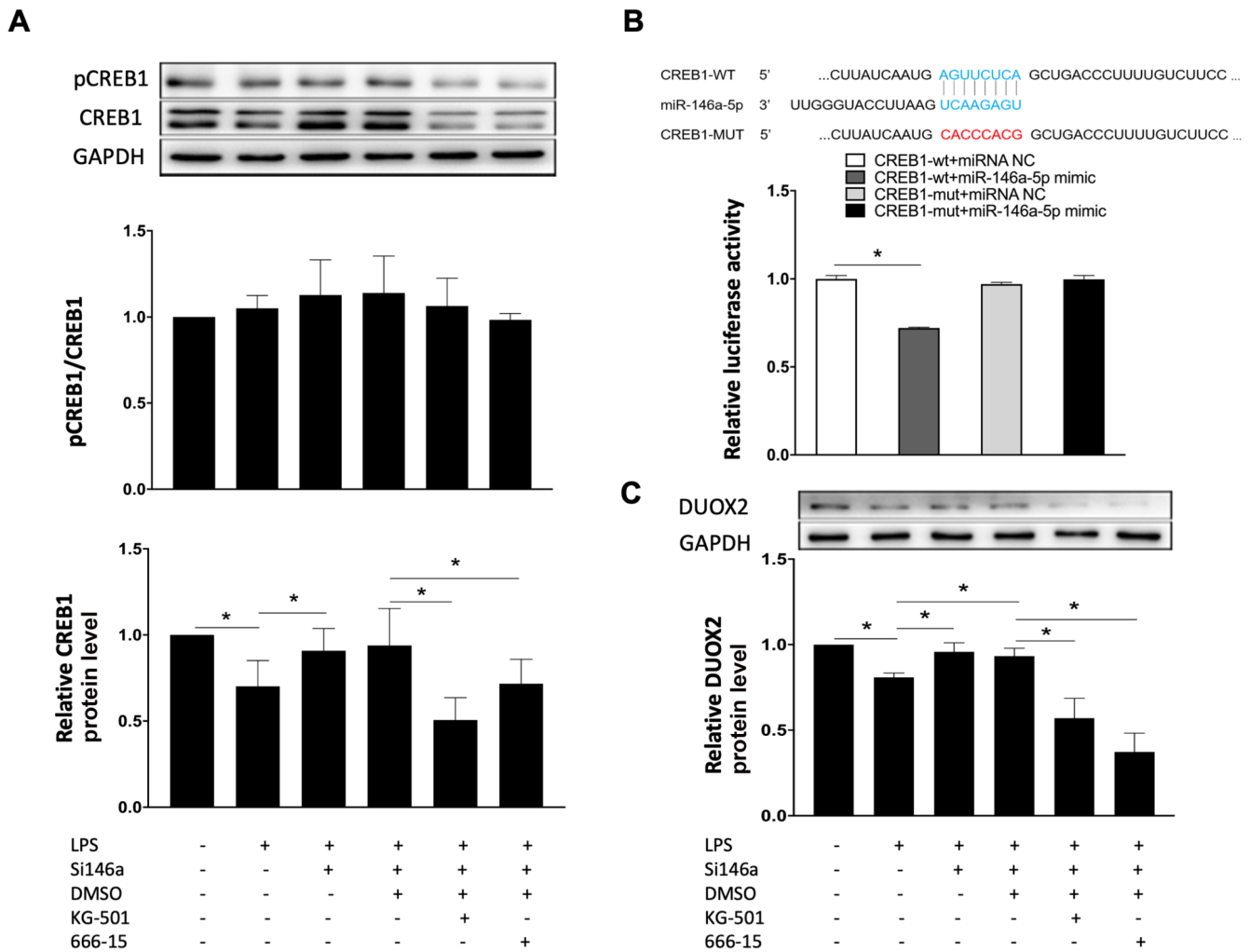
Figure 4. Mir-146a-5p regulates the expression of DUOX2 through the CREB1 pathway (A) The expression of CREB1 in telocytes was decreased when treated with LPS and increased when TCs were treated with antagomiR-146a-5p. AntagomiR-146a-5p restored CREB expression in the presence of LPS. (B) A dual-luciferase reporter assay revealed that the miR-146a-5p mimic significantly reduced the CREB1 promoter activity. (C) AntagomiR-146a-5p significantly increased DUOX2 protein expression in TCs compared with cells transfected with the negative control. In the presence of antagomiR-146a-5p and LPS, KG-501 and 666-15 significantly reduced DUOX2 protein expression. Data are shown as the mean $\pm$ standard deviation from six independent experiments ($n = 6$). *$P < 0.05$.

reduced DUOX2 protein expression (Figure 4C).

Family members of JAK/STAT are not involved in the expression of DUOX2 in TCs

After stimulation with LPS for 6 h, the levels of phosphorylated JAK1 and STAT3(Tyr705) were significantly increased (Figure 5A), but did not change after treatment with antagomiR-146a-5p (Figure 5B). LPS stimulation increased level of phosphorylated STAT1 on tyrosine 701 residue (Figure 5A), which was restored by antagomiR-146a-5p treatment, but it failed to change the expression of DUOX2 (Figure 5B).

Discussion

The present study reports that DUOX2 protein plays a vital role in the protective effect of TCs in the mouse ARDS model. After LPS stimulation, DUOX2 protein expression is decreased in mouse TCs, which is regulated by transcription factor CREB1. Enhanced ex-

pression of miR-146a-5p inhibits CREB1 transcription, resulting in reduced expression of DUOX2 protein as well as a decrease in oxidative stress.

The enzyme DUOX2, a member of the nicotinamide adenine dinucleotide phosphate (NADPH) family, has a peroxidase homology domain and a gp91phox domain [40]. Increased expression of DUOX2 has been reported in human pancreatic cancer cells when being exposed to IFN-γ [41]. In the present study, DUOX2 expression was found to be reduced in pulmonary TCs, but increased in RAW264.7 and MLE-12, suggesting that TCs exert distinguished antioxidative effects in response to LPS as well as in the mouse ARDS model.

DUOX2 protein is regulated at a transcriptional level. In cultured human pancreatic cells, interferon-gamma activates STAT1, with increased phosphorylation on tyrosine 701 residue, leading to the upregulation of DUOX2 protein [41,42]. In the present study, we found that LPS stimulation increased level of phosphorylated
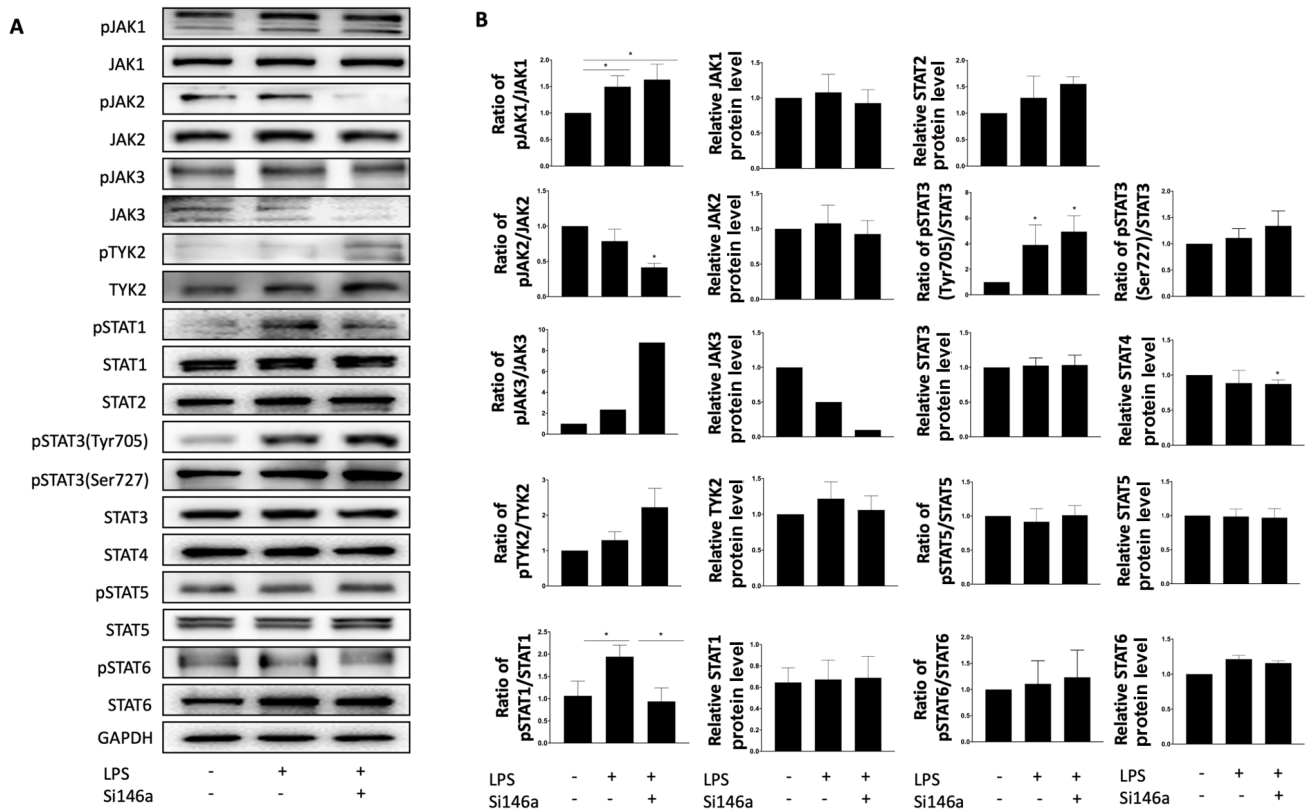
Figure 5. Phosphorylation of family members of JAK/STAT are upregulated after LPS stimulation in telocytes but are not related to the expression of DUOX2 (A) LPS significantly increased the levels of phosphorylated JAK1, STAT1, and STAT3. (B) The levels of phosphorylated JAK1 and STAT3 failed to be restored by antagomiR-146a-5p incubation, but the level of phosphorylated STAT1 was restored. Data are shown as the mean ± standard deviation from six independent experiments ($n = 6$). *$P < 0.05$.

STAT1 in TCs, but reduced DUOX2 expression, indicating that STAT1 does not regulate DUOX2 protein in TCs. CREB1 binds to the promoter of the DUOX2 gene. LPS stimulation reduced CREB1 protein expression, both the phosphorylated protein and total protein. Inhibition of expression of miR-146a-5p, in the presence of antagomiR-146a-5p in which CREB1 and DUOX2 expressions were restored, upregulated DUOX2 protein supporting the note that CREB1 regulates DUOX2 protein expression.

MicroRNAs (miRNAs), small non-coding ribonucleic acid molecules, regulate target genes by inhibiting mRNA translation or promoting mRNA degradation [43,44]. It has been proposed that miRNAs are potential therapeutic targets in acute lung injury [45], since miR-216a level is decreased in ARDS patients, and the reduced expression of miR-216a is negatively correlated with the mortality of ARDS patients, while overexpressing miR-216a decreases TNF α, IL-6, and IL-1 β levels in adenocarcinomic human alveolar basal epithelial A549 cells stimulated with LPS [46]. Inhibition of miR-26a disrupts human lung microvascular endothelial cells barrier via increasing the expression of Eph receptors EA2 [47]. Neutrophil-derived miR-223 accelerates acute lung injury by downregulating poly(ADP-ribose)polymerase-1 (PARP-1) protein [48]. MicroRNA-146a alleviates LPS-mediated inflammation in a mouse ARDS model by inhibiting protein expressions of interleukin-1 receptor-associated kinase 1 and TNF receptor-associated factor 6 [49,50]. MicroRNA-21a-3p promotes angiogenesis in endothelial cells under inflammatory conditions by regulating E2F8-Notch2 protein expressions [20,28]. In the present study, miR-146a-5p is found to

regulate CREB1 protein expression by binding with its promoter, leading to decreased expression of DUOX2 protein, indicating that miR-146a-5p exerts beneficial effects by downregulating oxidative enzymes in TCs.

In conclusion, miR-146a-5p in TCs downregulates the expression of DUOX2 via the CREB1 pathway and administration of TCs protects the function of the lung undergoing oxidative stress damage (Figure 6).
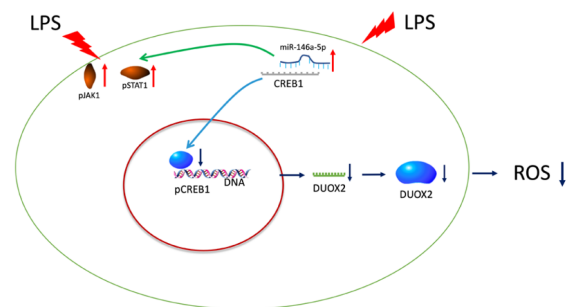

Figure 6. Schematic diagram of the pathway of DUOX2 production controlled by miR-146a-5p LPS-induced DUOX2 production was decreased through the miR-146a-5p/CREB1/DUOX2 signaling pathway in TCs. TC, telocyte; ROS, reactive oxygen species; LPS, lipopolysaccharide; JAK, janus kinase; STAT, signal transducer and activator of transcription; DUOX2, dual oxidase 2; and CREB1, cAMP-response element binding protein 1.

Conflict of Interest

The authors declare that they have no conflict of interest.

References

1. Matthay MA, Zemans RL, Zimmerman GA, Arabi YM, Beitler JR, Mercat A, Herridge M, et al. Acute respiratory distress syndrome. *Nat Rev Dis Primers* 2019, 5: 18
2. Diamond M, Peniston Feliciano HL, Mahapatra S. Acute Respiratory Distress Syndrome (ARDS). StatPearls Publishing LLC., Treasure Island (FL), 2019
3. Dong Z, Yuan Y. Accelerated inflammation and oxidative stress induced by LPS in acute lung injury: lnhibition by ST1926. *Int J Mol Med* 2018, 41: 3405–3421
4. Butt Y, Kurdowska A, Allen TC. Acute lung injury: a clinical and molecular review. *Arch Pathol Laboratory Med* 2016, 140: 345–350
5. Máca J, Jor O, Holub M, Sklienka P, Burša F, Burda M, Janout V, et al. Past and present ARDS mortality rates: a systematic review. *Respiratory Care* 2017, 62: 113–122
6. Gerloff J, Sundar IK, Freter R, Sekera ER, Friedman AE, Robinson R, Pagano T, et al. Inflammatory response and barrier dysfunction by different e-cigarette flavoring chemicals identified by gas chromatography–mass spectrometry in e-liquids and e-vapors on human lung epithelial cells and fibroblasts. *Appl Vitro Toxicol* 2017, 3: 28–40
7. Peters S, Kronseder A, Karrasch S, Neff PA, Haaks M, Koczulla AR, Reinhold P, et al. Hydrogen peroxide in exhaled air: a source of error, a paradox and its resolution. *ERJ Open Res* 2016, 2: 00052-2015
8. Liu D, Luo G, Luo C, Wang T, Sun G, Hei Z. Changes in the concentrations of mediators of inflammation and oxidative stress in exhaled breath condensate during liver transplantation and their relations with postoperative ARDS. *Respiratory Care* 2015, 60: 679–688
9. Zhang S, Wang P, Zhao P, Wang D, Zhang Y, Wang J, Chen L, et al. Pretreatment of ferulic acid attenuates inflammation and oxidative stress in a rat model of lipopolysaccharide-induced acute respiratory distress syndrome. *Int J Immunopathol Pharmacol* 2018, 31: 039463201775051
10. Popescu LM, Faussone-Pellegrini MS. TELOCYTES - a case of serendipity: the winding way from Interstitial Cells of Cajal (ICC), via Interstitial Cajal-Like Cells (ICLC) to TELOCYTES. *J Cell Mol Med* 2010, 14: 729–740
11. Zheng Y, Li H, Manole CG, Sun A, Ge J, Wang X. Telocytes in trachea and lungs. *J Cell Mol Med* 2011, 15: 2262–2268
12. Cretoiu D, Cretoiu SM. Telocytes in the reproductive organs: current understanding and future challenges. *Semin Cell Dev Biol* 2016, 55: 40–49
13. Cretoiu D, Radu BM, Banciu A, Banciu DD, Cretoiu SM. Telocytes heterogeneity: from cellular morphology to functional evidence. *Semin Cell Dev Biol* 2017, 64: 26–39
14. Kostin S. Myocardial telocytes: a specific new cellular entity. *J Cell Mol Med* 2010, 14: 1917–1921
15. Shoshkes-Carmel M, Wang YJ, Wangensteen KJ, Tóth B, Kondo A, Massasa EE, Itzkovitz S, et al. Subepithelial telocytes are an important source of Wnts that supports intestinal crypts. *Nature* 2018, 557: 242–246
16. Cretoiu D, Cretoiu SM, Simionescu AA, Popescu LM. Telocytes, a distinct type of cell among the stromal cells present in the lamina propria of jejunum. *Histol Histopathol* 2012, 27: 1067–1078
17. Song D, Cretoiu D, Cretoiu SM, Wang X. Telocytes and lung disease. *Histol Histopathol* 2016, 31: 1303–1314
18. Hussein MM, Mokhtar DM. The roles of telocytes in lung development and angiogenesis: an immunohistochemical, ultrastructural, scanning electron microscopy and morphometrical study. *Dev Biol* 2018, 443: 137–152
19. Li L, Lin M, Li L, Wang R, Zhang C, Qi G, Xu M, et al. Renal telocytes contribute to the repair of ischemically injured renal tubules. *J Cell Mol Med* 2014, 18: 1144–1156
20. Ma R, Wu P, Shi Q, Song D, Fang H. Telocytes promote VEGF expression and alleviate ventilator-induced lung injury in mice. *Acta Biochim Biophys Sin* 2018, 50: 817–825
21. Zhao B, Liao Z, Chen S, Yuan Z, Yilin C, Lee KKH, Qi X, et al. Intramyocardial transplantation of cardiac telocytes decreases myocardial infarction and improves post-infarcted cardiac function in rats. *J Cell Mol Med* 2014, 18: 780–789
22. Zheng Y, Cretoiu D, Yan G, Cretoiu SM, Popescu LM, Wang X. Comparative proteomic analysis of human lung telocytes with fibroblasts. *J Cell Mol Med* 2014, 18: 568–589
23. Zheng Y, Cretoiu D, Yan G, Cretoiu SM, Popescu LM, Fang H, Wang X. Protein profiling of human lung telocytes and microvascular endothelial cells using iTRAQ quantitative proteomics. *J Cell Mol Med* 2014, 18: 1035–1059
24. Zheng M, Sun X, Zhang M, Qian M, Zheng Y, Li M, Cretoiu SM, et al. Variations of chromosomes 2 and 3 gene expression profiles among pulmonary telocytes, pneumocytes, airway cells, mesenchymal stem cells and lymphocytes. *J Cell Mol Med* 2014, 18: 2044–2060
25. Ye L, Song D, Jin M, Wang X. Therapeutic roles of telocytes in OVA-induced acute asthma in mice. *J Cell Mol Med* 2017, 21: 2863–2871
26. Zhang D, Song D, Shi L, Sun X, Zheng Y, Zeng Y, Wang X. Mechanisms of interactions between lung-origin telocytes and mesenchymal stem cells to treat experimental acute lung injury. *Clin Transl Med* 2020, 10: e231
27. Albulescu R, Tanase C, Codrici E, Popescu DI, Cretoiu SM, Popescu LM. The secretome of myocardial telocytes modulates the activity of cardiac stem cells. *J Cell Mol Med* 2015, 19: 1783–1794
28. Zhou Y, Yang Y, Liang T, Hu Y, Tang H, Song D, Fang H. The regulatory effect of microRNA-21a-3p on the promotion of telocyte angiogenesis mediated by PI3K (p110α)/AKT/mTOR in LPS induced mice ARDS. *J Transl Med* 2019, 17: 427
29. Wang L, Song D, Wei C, Chen C, Yang Y, Deng X, Gu J. Telocytes inhibited inflammatory factor expression and enhanced cell migration in LPS-induced skin wound healing models *in vitro and in vivo*. *J Transl Med* 2020, 18: 60
30. Song D, Xu M, Qi R, Ma R, Zhou Y, Wu D, Fang H, et al. Influence of gene modification in biological behaviors and responses of mouse lung telocytes to inflammation. *J Transl Med* 2019, 17: 158
31. Cismașiu VB, Popescu LM. Telocytes transfer extracellular vesicles loaded with microRNAs to stem cells. *J Cell Mol Med* 2015, 19: 351–358
32. Cretoiu D, Xu J, Xiao J, Cretoiu SM. Telocytes and their extracellular vesicles—evidence and hypotheses. *Int J Mol Sci* 2016, 17: 1322
33. Afonso-Grunz F, Müller S. Principles of miRNA–mRNA interactions: beyond sequence complementarity. *Cell Mol Life Sci* 2015, 72: 3127–3141
34. Huang Y. The novel regulatory role of lncRNA-miRNA-mRNA axis in cardiovascular diseases. *J Cell Mol Med* 2018, 22: 5768–5775

35. Kim DH, Chung JH, Son BS, Kim YJ, Lee SG. Effect of a neutrophil elastase inhibitor on ventilator-induced lung injury in rats. *J Thorac Dis* 2014, 6:12, 1681–1689

36. Cheng X, He S, Yuan J, Miao S, Gao H, Zhang J, Li Y, *et al.* Lipoxin A4 attenuates LPS-induced mouse acute lung injury via Nrf2-mediated E-cadherin expression in airway epithelial cells. *Free Radical Biol Med* 2016, 93: 52–66

37. Li Y, Huang J, Foley NM, Xu Y, Li YP, Pan J, Redmond HP, *et al.* B7H3 ameliorates LPS-induced acute lung injury via attenuation of neutrophil migration and infiltration. *Sci Rep* 2016, 6: 31284

38. Song D, Tang L, Wang L, Huang J, Zeng T, Fang H, Wang X. Roles of TGFβ1 in the expression of phosphoinositide 3-kinase isoform genes and sensitivity and response of lung telocytes to PI3K inhibitors. *Cell Biol Toxicol* 2020, 36: 51–64

39. Fanunza E, Frau A, Sgarbanti M, Orsatti R, Corona A, Tramontano E. Development and validation of a novel dual luciferase reporter gene assay to quantify Ebola virus VP24 inhibition of IFN signaling. *Viruses* 2018, 10: 98

40. Harper RW, Xu C, Eiserich JP, Chen Y, Kao CY, Thai P, Setiadi H, *et al.* Differential regulation of dual NADPH oxidases/peroxidases, Duox1 and Duox2, by Th1 and Th2 cytokines in respiratory tract epithelium. *FEBS Lett* 2005, 579: 4911–4917

41. Wu Y, Antony S, Juhasz A, Lu J, Ge Y, Jiang G, Roy K, *et al.* Up-regulation and sustained activation of stat1 are essential for interferon-γ (ifn-γ)-induced dual oxidase 2 (duox2) and dual oxidase a2 (duoxa2) expression in human pancreatic cancer cell lines. *J Biol Chem* 2011, 286: 12245–12256

42. Wu Y, Antony S, Hewitt SM, Jiang G, Yang SX, Meitzler JL, Juhasz A, *et al.* Functional activity and tumor-specific expression of dual oxidase 2 in pancreatic cancer cells and human malignancies characterized with a novel monoclonal antibody. *Int J Oncol* 2013, 42: 1229–1238

43. Wang JY, Yang Y, Ma Y, Wang F, Xue A, Zhu J, Yang H, *et al.* Potential regulatory role of lncRNA-miRNA-mRNA axis in osteosarcoma. *Biomed PharmacoTher* 2020, 121: 109627

44. Mellis D, Caporali A. MicroRNA-based therapeutics in cardiovascular disease: screening and delivery to the target. *Biochem Soc Trans* 2018, 46: 11–21

45. Rajasekaran S, Pattarayan D, Rajaguru P, Sudhakar Gandhi PS, Thimmulappa RK. MicroRNA regulation of acute lung injury and acute respiratory distress syndrome. *J Cell Physiol* 2016, 231: 2097–2106

46. Kong F, Sun Y, Song W, Zhou Y, Zhu S. MiR-216a alleviates LPS-induced acute lung injury via regulating JAK2/STAT3 and NF-κB signaling. *Hum Cell* 2020, 33: 67–78

47. Good RJ, Hernandez-Lagunas L, Allawzi A, Maltzahn JK, Vohwinkel CU, Upadhyay AK, Kompella UB, *et al.* MicroRNA dysregulation in lung injury: the role of the miR-26a/EphA2 axis in regulation of endothelial permeability. *Am J Physiol-Lung Cell Mol Physiol* 2018, 315: L584–L594

48. Neudecker V, Brodsky KS, Clambey ET, Schmidt EP, Packard TA, Davenport B, Standiford TJ, *et al.* Neutrophil transfer of *miR-223 to lung epithelial cells dampens acute lung injury in mice. Sci Transl Med* 2017, 9: eaah5360

49. Zeng Z, Gong H, Li Y, Jie K, Ding C, Shao Q, Liu F, *et al.* Upregulation of miR-146a contributes to the suppression of inflammatory responses in LPS-induced acute lung injury. *Exp Lung Res* 2013, 39: 275–282

50. Wu H, Fan H, Shou Z, Xu M, Chen Q, Ai C, Dong Y, *et al.* Extracellular vesicles containing miR-146a attenuate experimental colitis by targeting TRAF6 and IRAK1. *Int ImmunoPharmacol* 2019, 68: 204–212